

المجلة العلمية

لجامعة إقليم سبأ

مجلة علمية نصفية محكّمة

تصدر عن جامعة إقليم سبأ

ISSN :2709-2747 (Online)

ISSN :2709-2739 (Print)

المجلد (9) - العدد (2) - سبتمبر 2026م

Scientific Journal
University of Saba Region
ISSN :2709- 2747 (Online)

المجلة العلمية
لجامعة إقليم سبأ
ISSN :2709- 2739 (Print)

تحليل الاستقرار والحساسية لمرشّح شامل مبتكر يعمل بنمط الجهد، قائم على المكثفات المبدَّلة

AN INNOVATIVE VOLTAGE-MODE UNIVERSAL SWITCHED-CAPACITOR FILTER: STABILITY AND SENSITIVITY ANALYSIS

عدنان عبدالله قاسم أبوبكر [1]
Adnan Abdullah Qasem Abobakr

تاريخ استلام البحث	تاريخ قبول البحث
2026/6/19م	2026/7/30م

المجلد(9) العدد(2) سبتمبر 2026م
https://doi.org/10.54582/TSJ.2.2.170

(1) أستاذ الفيزياء المساعد، كلية التربية والعلوم، جامعة إقليم سبأ.
عنوان المراسلة : Dr.A.Q.Adnan@usr.edu.ye

الملخص:

يقدّم هذا العمل مرشح شامل ذو بنية مبتكرة، ويعمل بنمط الجهد، إلى جانب دراسة استجابة استقراره ضمن تشكيلة بنيوية جديدة. ومن خلال التعديل الملائم لفروع خرج الجهد لمضخمات العمليات (op-amps)، يمكن للدائرة تحقيق طيف واسع من دوال التمرير (التمرير المنخفض، والتمرير النطاقي، والتمرير العالي) في دائرة واحدة. كما يمكن استخدام الدائرة كمرشح تمرير نطاقي ضيق وكمرشح تمرير نطاقي عريض على حدٍ سواء. وتُظهر النتائج أن الدائرة تؤدي أداءً محسنًا في نطاق التمرير النطاقي (band-pass) لكافة مستويات عامل الجودة (Q-factor) وترددات المركز. كما تبيّن النتائج أن الدائرة تحقق أداءً أفضل في حالات عامل الجودة (Q=1) ضمن نطاقي التمرير المنخفض والتمرير العالي. وتتميز الدائرة بحساسية منخفضة تجاه العناصر الفعَّالة والغير فعَّالة على حَدٍّ سواء. هذا وتُستحصَل دوال الخرج (التمرير المنخفض، والتمرير النطاقي، والتمرير العالي) في آنٍ واحد ضمن دائرة واحدة. وتكمن ميزة استجابة الاستقرار في مرشحات من نوع RC في ضمان بقاء إشارة الخرج ضمن نطاق محدد، وعدم تعرضها للتموج أو التباعد بمرور الزمن، فضلاً عن الاستغناء عن المكونات الغير فعَّالة، مما قد يسهم في تقليص حجم الرقاقة المطلوبة لتنفيذ الدوائر المتكاملة (IC). وتُستخدم المرشحات من نوع RC في قطاعات صناعية متعددة، تشمل الاتصالات، والسيارات، والطب، والإلكترونيات الاستهلاكية. وقد تم التحقق من النتائج النظرية، باستخدام برنامج محاكاة الدوائر الإلكترونية من نوع PSPICE.

الكلمات المفتاحية: استجابة الاستقرار، نظام من الدرجة الثالثة، نمط الجهد، معامل الجودة، مرشح نشط.

Abstract

This work presents an innovative voltage-mode universal switched-capacitor filter and its stability response in a novel configuration. By appropriately altering the voltage-output branches of op-amps, the circuit can implement a variety of transfer functions (low-pass (LP), band-pass (BP), and high-pass (HP)) in single circuit. The circuit can be used as narrow band-pass as well as wide band-pass filter. For all Q-factor and center frequency levels, the circuit performs better in terms of band-pass. The findings demonstrate that the circuit performs better for Q=1 in the low-pass (LP) and high-pass (HP) ranges. Low sensitivity to active and passive elements characterizes the circuit. The output functions: LP, BP, and HP are getting simultaneously in single circuit. The benefit of RC-filter's stability response is that it makes sure the output signal stays within a specific range and doesn't fluctuate or diverge over time and the removal of passive components, which could reduce the chip size needed for integrated circuit (IC) implementations. The RC-filters are used in many different industries including telecommunications, automotive, medical, and consumer electronics. The theoretical results are verified using PSPICE circuit simulation program.

Keywords: Stability Response, Third-Order, Voltage-Mode, Merit Factor, Active Filter.

Copyright: © 2026 Faisal Mohammed Ali Al-Qubati. This article is an open-access article distributed under the terms and conditions of Creative Commons Attribution (CC BY 4.0) license.

1.0 INTRODUCTION

A filter's capacity to maintain a constant output signal despite changes in the input signal or other outside influences is known as its stability response. An unstable filter may result in irregular or unpredictable outputs, whereas a stable filter will yield a predictable and trustworthy output. The transfer function of a filter, which represents the connection between the input and output signals, is often analysed in order to determine the stability response of the filter. The design of the filter circuit, the properties of the components utilized in the circuit, and external conditions like temperature or electromagnetic interference are all variables that might alter a filter's stability response. The fundamental idea behind a switched capacitor is to replace resistors with capacitors and analog switches. After replacing the resistor with an op-amp-based integrator, an active filter is created (1999, Grise). Digital and analog functionality may now be combined on a single silicon chip thanks to switched capacitor technology. In most instances, switched-capacitor filters offer the advantage of greater precision. The worst-case estimates vary from 0.4% to 1.5%, with typical center frequency accuracies of around 0.2% for switched-capacitor ICs (assuming, of course, that an accurate clock is given) (2010, Shinde& Bhagat). The implementation of resistors was a significant barrier to the production of filters on chips, but the Switched-Capacitor technology overcame this by imitating resistors with high-speed Switched-Capacitors utilizing MOSFETs. The filter responds discretely rather than continuously as a result of the MOSFET's switching function (2010, Shinde& Bhagat). The transfer function of filter circuits is determined using the ratio of resistances in conventional analog circuits. The frequency responses of these circuits

are controlled by the values of the RC product (2008, Shinde& Bhagat). In terms of compactness, simplicity of design, and expansion of response towards high frequencies, active filters using simply resistors have numerous benefits (2002, Shinde& Patil, Kadam, Mirkute). On a single chip, they may be integrated with digital circuitry (2006, Senani& Gupta). Building blocks for switched–capacitor (SC) systems are frequently divided into two groups: passive and active. A network made of just of switches and capacitors is referred to as a passive SC building block (or element), whereas an active network includes active components like op–amps in addition to switches and capacitors. A MOS switch is technically an active device since it has one or more transistors that require the system clock or its derivatives to drive them (2006, Liu). Designing a filter using different active building blocks (ABBs), such as voltage differencing buffered amplifier (VDBA) (2012, Kacar& Yesil, Noori), four terminal floating nullor (FTFN) (2018, Tarunkumar& Ranjan, Pheiroijam), current differencing buffered amplifier (CDBA) (2013, Pathak& Singh, Senani), differential difference current conveyor (DDCC) (2017, Yuce), voltage differencing current conveyor (VDCC) (2021, Roy), and differential voltage current conveyor (DVCC) (2013, Horng& Jhao), has recently attracted more attention. Using operational amplifiers (OAs) and four capacitors with MOSFETs, this paper describes a novel circuit architecture for implementing an electrically adjustable 3rd–order voltage–mode switched–capacitor (SC) filter. Different values of the center frequency f_o and Q–factor have been explored for this circuit architecture, circuit analysis, and constructed equations. Op–amps, passive components, and single–input multiple–output signals are used in the demonstrated circuit. An alternative to a resistor is a switched–

capacitor (1984, Ghausi). Switched-capacitor circuits may be designed using MOSFET technology (2006, Shah& Rather, Iqbal). It is possible to create extremely complex, precise, and adjustable analog circuits utilizing switched-capacitor filter circuits. The benefit of RC-filter's stability response is that it makes sure the output signal stays within a specific range and doesn't fluctuate or diverge over time. This is crucial for a variety of applications that demand a consistent output signal, including audio processing, control systems, and communication systems. Additionally, a consistent filter response guarantees that the filter won't add any unwanted noise or distortion to the signal. Furthermore, a stable RC-filter response makes it simpler to analyze and build the filter since it eliminates mistakes in calculations and lowers the possibility of instability problems.

1.1 BASIC SWITCHING OPERATION

The circuit schematic that follows may be used to show how the switched-capacitor works:

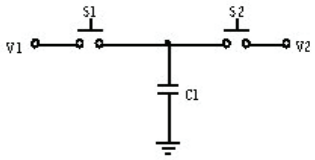

Fig. 1. 1: An illustration of the switched-capacitor's circuitry.

Since the charge q on a capacitor $\mathcal{C}_1$ is given by

$$q = \mathcal{C}_1 \mathcal{V} \qquad (1.1)$$

$\mathcal{V}$, however, represents the voltage across the $\mathcal{C}_s$. capacitor. Consequently, a charge q is transferred from $\mathcal{V}_2$ to $\mathcal{V}_1$ with S_1 closing after S_2 closes with S_2 open.

$$\Delta q = \mathcal{C}_1 (\mathcal{V}_2 - \mathcal{V}_1) \qquad (1.2)$$

The quantity of charge transferred per unit time is given by if this switching procedure is performed N times in time (τ).

$$\frac{\Delta q}{\Delta \tau} = \mathcal{C}_1(\mathcal{V}_2 - \mathcal{V}_1)\frac{N}{\Delta \tau} \qquad (1.3)$$

The number of cycles per unit of time is the switching frequency, and L.H.S. is the current.

$$\therefore i = \mathcal{C}_1(\mathcal{V}_2 - \mathcal{V}_1)\, f_{clk} \qquad (1.4)$$

$$\therefore \frac{(\mathcal{V}_2 - \mathcal{V}_1)}{i} = \frac{1}{\mathcal{C}_1 f_{clk}} = R \qquad (1.5)$$

The switched capacitor is therefore comparable to a resistor.

1.2 CIRCUIT CONFIGURATION BEING PROPOSED

Fig. 1.2 depicts the suggested circuit layout for implementing an electrically adjustable 3rd–order voltage–mode switched–capacitor circuit. Only three op–amps and four capacitors with MOSFETs make up the circuit, which forms a switching capacitor. Through a switched–capacitor (SC_4), the input low–voltage signal is supplied to first and second operation–inverting amplifiers' terminal.

The first op–amp's non–inverting terminal is grounded. The second operation–non–inverting input receives the first op– amplifier's output. It uses SC_1 as feedback. The third op–amp's non–inverting input receives the output of the second op–amp. The third operation–inverting amplifier's terminal is grounded. As feedback, SC_2 and SC_4 are employed. At the output of the third and second op–amps, respectively, the low pass and band pass transfer functions are visible. The first op–amp's inverting input displays the high pass transfer function.

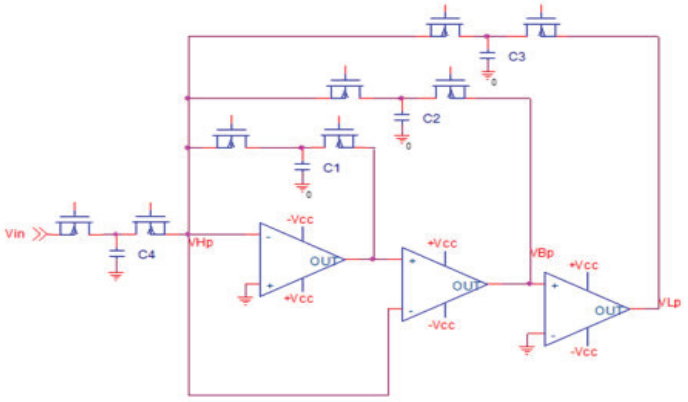

Fig. 1. 2: Circuit diagram of an innovative voltage–mode universal switched–capacitor filter.

1.3 CIRCUIT ANALYSIS AND DESIGN EQUATIONS

Internally compensated op–amps, such as the AD8622, are represented by a "single pole model":

$$A(s) = (A_0\omega_0/(s + \omega_0)) \qquad (1.6)$$

Where,

Open loop: A_0 D.C gain, ω_0=open loop –3dB bandwidth, $\epsilon = A_0\omega_0$= gain bandwidth product of op–amplifier, and S is the complex frequency variable.

$$A(s) = (A_0\omega_0/s) = \epsilon_i/s \text{ where i} = 1, 2, 3, \ldots (1.7)$$

Where, S >> ω_0

The op–amp is clearly an "integrator" in light of this. As a result, three distinct nodes of a unique voltage–mode universal RC–filter transfer function as follows:

The low pass filter's voltage transfer function is provided by:

$$T(S)_{LP} = \frac{-\epsilon_1\epsilon_2\epsilon_3\mathcal{C}_4}{\lambda_1 S^3 + \lambda_2 S^2 + \lambda_3 S + \lambda_4} \qquad (1.8)$$

The band pass filter's voltage transfer function is provided by:

$$T(S)_{BP} = \frac{-S\epsilon_1\epsilon_2\mathcal{C}_4}{\lambda_1 S^3 + \lambda_2 S^2 + \lambda_3 S + \lambda_4} \qquad (1.9)$$

The high pass filter's voltage transfer function is provided by:

$$T(S)_{HP} = \frac{S^3\mathcal{C}_4}{\lambda_1 S^3 + \lambda_2 S^2 + \lambda_3 S + \lambda_4} \qquad (1.10)$$

Where

$\lambda_1 = \mathcal{C}_1 + \mathcal{C}_2 + \mathcal{C}_3 + \mathcal{C}_4$ $\qquad$ $\lambda_3 = \epsilon_1\epsilon_2\mathcal{C}_2 + \epsilon_2\epsilon_3\mathcal{C}_3$

$\lambda_2 = \epsilon_1\mathcal{C}_1 + \epsilon_2\mathcal{C}_2$ $\qquad$ $\lambda_4 = \epsilon_1\epsilon_2\epsilon_3\mathcal{C}_3$

The coefficient-matching technique (CMT) method is used to create the circuit, by comparing the coefficients of denominator of the transfer function with the coefficients of denominator of the general 3rd-order transfer function. The general 3rd-order transfer function is given by:

$$T(s) = \frac{\zeta_3 S^3 + \zeta_2 S^2 + \zeta_1 S + \zeta_0}{S^3 + \omega_0\left(1 + \frac{1}{Q}\right)S^2 + \omega_0^2\left(1 + \frac{1}{Q}\right)S + \omega_0^3} \qquad (1.11)$$

We get the design equations as:

$\mathcal{C}_1 + \mathcal{C}_2 + \mathcal{C}_3 + \mathcal{C}_4 = 1$ (1.12)

$\epsilon_1\mathcal{C}_1 + \epsilon_2\mathcal{C}_2 = \omega_0(1 + 1/Q)$ (1.13)

$\epsilon_1\epsilon_2\mathcal{C}_2 + \epsilon_2\epsilon_3\mathcal{C}_3 = \omega_0^2(1 + 1/Q)$ (1.14)

$\epsilon_1\epsilon_2\epsilon_3\mathcal{C}_3 = \omega_0^3$ (1.15)

These equations may be used to determine the values of $\mathcal{C}_1, \mathcal{C}_2, \mathcal{C}_3$ *and* $\mathcal{C}_4$ for various Q-factor and central frequency f_O values.

1.4 SENSITIVITY

The parameter-specific $\mathcal{C}_1, \mathcal{C}_2, \mathcal{C}_3, \mathcal{C}_4, \epsilon_1, \epsilon_2$ and ϵ_3 passive and

https://doi.org/10.54582/TSJ.2.2.170

active sensitivities

are as the following:

1.4.1 ω_0 Sensitivities

$$S_{C_1}^{\omega_0} = -\frac{1}{3}C_1 \quad (1.16)$$

$$S_{C_2}^{\omega_0} = -\frac{1}{3}C_2 \quad (1.17)$$

$$S_{C_3}^{\omega_0} = -\frac{1}{3}\{C_3 - 1\} \quad (1.18)$$

$$S_{C_4}^{\omega_0} = -\frac{1}{3}C_4 \quad (1.19)$$

$$S_{\epsilon_1}^{\omega_0} = S_{\epsilon_2}^{\omega_0} = S_{\epsilon_3}^{\omega_0} = \frac{1}{3} \quad (1.20)$$

1.4.2 Q –factor Sensitivities

$$S_{C_1}^{Q} = -\frac{1}{3}(1+Q)C_1 \quad (1.21)$$

$$S_{V_2}^{Q} = -(1+Q)C_2\left\{\frac{1}{(C_2+C_3)} - \frac{1}{3}\right\} \quad (1.22)$$

$$S_{C_3}^{Q} = -(1+Q)C_3\left\{\frac{1}{(C_2+C_3)} - \frac{1}{3} - \frac{2}{3C_3}\right\} \quad (1.23)$$

$$S_{C_4}^{Q} = -\frac{1}{3}(1+Q)\,C_4 \quad (1.24)$$

$$S_{\epsilon_1}^{Q} = -(1+Q)\left\{\frac{C_2}{C_2+C_3} - \frac{2}{3}\right\} \quad (1.25)$$

$$S_{\epsilon_2}^{Q} = -\frac{1}{3}(1+Q) \quad (1.26)$$

$$S_{\epsilon_3}^{Q} = -(1+Q)\left\{\frac{C_3}{C_2+C_3} - \frac{2}{3}\right\} \quad (1.27)$$

A unique voltage–mode universal RC–filter circuit's passive and active sensitivities are all below unity as a result. Since these sensitivities are so low, the circuit is, in real actuality, stable.

1.5 RESULTS AND DISCUSSION

The results of an experimental evaluation of an innovative voltage–mode universal switched–capacitor filter at the low–pass (LP), band–

pass (BL), and high-pass (HP) output terminals are shown below. An innovative voltage-mode universal RC-filter was built and simulated using the PSPICE circuit simulation tool to validate the theoretical work.

1.5.1 An innovative voltage-mode universal switched-capacitor filter's response to varying Q-factor

The circuit performance for low-pass (LP), band-pass (BP), and high-pass (HP) filters is investigated for various values of Q-factor with a certain value of the circuit central frequency. This circuit's normal working range is between 10 Hz and 1.2 MHz. The value of ϵ ($\epsilon_1 = \epsilon_1 = \epsilon_1$) is $2\pi\ (0.56) \times 10^6\ rad/sec$.

Table 1. 1: Capacitors values for low-pass (LP) filter, with $f_o = 220\ kHz$.

Q	C_1 (µf)	C_2 (µf)	C_3 (µf)	C_4 (µf)
1	53.8	24.8	6.06	15.4
2	41.8	17.1	6.06	35.01
4	35.9	13.2	6.06	44.8
8	32.9	11.3	6.06	49.7
10	32.3	10.9	6.06	50.7
20	31.1	10.1	6.06	52.7

Table 1. 2: Capacitors values for band-pass (BP) and high-pass (HP) filters,
with $f_o = 20\ kHz$.

Q	C_1 (µf)	C_2 (µf)	C_3 (nf)	C_4 (µf)
0.1	37.9	1.4	4.6	60.7
0.5	10.34	0.38	4.6	89.3
1	6.9	0.25	4.6	92.9
5	4.14	0.149	4.6	95.7
10	3.8	0.136	4.6	96.1
20	3.6	0.129	4.6	96.3

A. Low-Pass Filter Stability Response

A low-pass (LP) filter's stability response for various quality factor Q values is shown in Fig. 1.3. The details discovered by looking at the stability response curves in Fig. 1.3 is presented in Table 1.3. For $f_o = 220\ kHz$, the response is examined with quality factors of (0.1, 0.5, 1, 5, 10, and 20). For Q ≥1, the low-pass filter is effective. A low-pass filter's stability response for Q=1 reveals a gain margin of 1.47 dB at 311 kHz. The low-pass filter is thus only asymptotically stable for Q=1 with $f_o = 220\ kHz$. Additionally, it displays the phase margin of 7.31^0 for Q=1 at 292 kHz. For Q=1, the max gain is 8.1 dB at 0.44 kHz.

المجلد(9) العدد(2) سبتمبر 2026م
https://doi.org/10.54582/TSJ.2.2.170

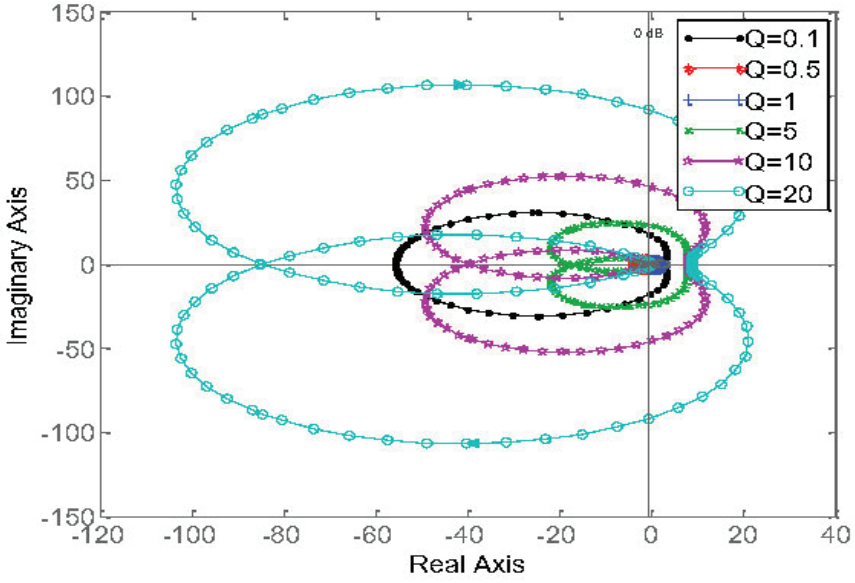

Fig. 1.3: Low-pass (LP) filter stability response, with $f_o = 220\,kHz$.

Table 1. 3: Low-pass (LP) response graph analysis of Fig. 1.3.

Q	Gain-Margin (G_M)		Phase-Margin (P_M)		Peak-Gain		Stability Status
	(dB)	f_{GCO} (kHz)	(deg)	f_{PCO} (kHz)	(dB)	f_P (kHz)	
0.1	-34.9	0	-166	493	34.9	4.44×10^{-11}	NW
0.5	-11.9	0	-152	269	11.9	4.4×10^{-10}	NW
1	1.47	311	7.31	292	8.1	0.44	S
5	-	241	-	457	28.	220	NS

		n			.4		
10	Inf	Na n	2.3	549	74 .3	20	S
20	Inf	Na n	2.19	550	79 .8	20	S

C. High–Pass Filter Stability Response

For a range of quality factor Q values, a high–pass (HP) filter's stability response is shown in Fig. 1.5. Table 1.5 contains the data that was discovered through the analysis of the stability response curves shown in Fig. 1.5. For $f_o = 20\ kHz$, the high–pass filter is investigated for various quality factor values (0.1, 0.5, 1, 5, 10, and 20). For all Q–Factor values, the high–pass filter is effective.

The gain margin is seen to only have a positive value for Q ≤ 1. For example, for Q = 0.1, it is 45.9 dB at 6.03 kHz, while for Q = 1, it is 10.2 dB at 14.1 kHz. With $f_o = 20\ kHz$, the high–pass filter is thus only asymptotically stable for Q ≤ 1. A high–pass filter's stability response demonstrates that Q ≤ 1 has an infinite phase margin. As the importance of the quality component rises, the peak gain rises. Thus, the gain margin, phase margin, and peak gain are all under the control of the quality factor.

المجلد(9) العدد(2) سبتمبر 2026م
https://doi.org/10.54582/TSJ.2.2.170

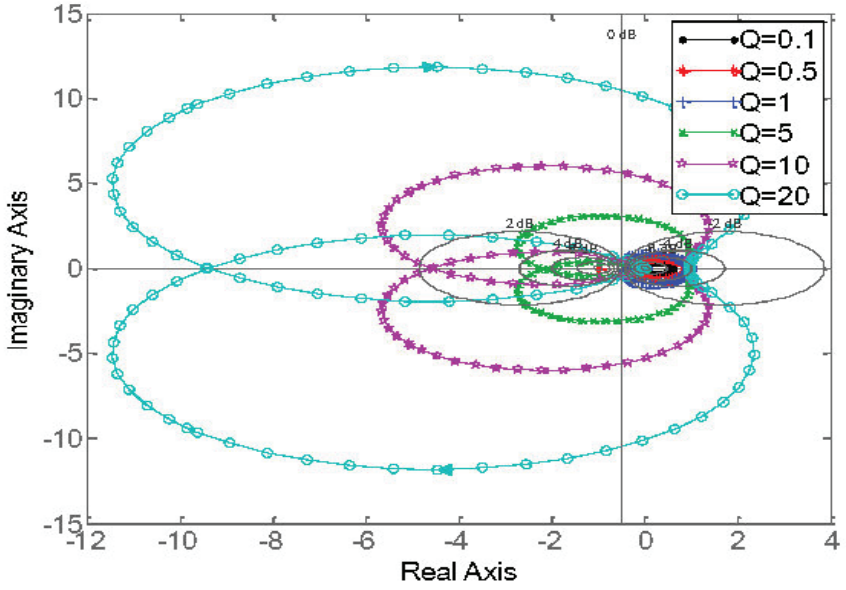

Fig. 1.5: High-pass (HP) filter stability response, with $f_O = 20\ kHz$.

Table 1. 5: High-pass (HP) response graph analysis of Fig. 1.5.

Q	Gain-Margin (G_M)		Phase-Margin (P_M)		Peak-Gain		Stability Status
	(dB)	f_{GCO} (kHz)	(deg)	f_{PCO} (kHz)	(dB)	f_P (kHz)	
0.1	45.9	6.03	Inf	Nan	−4.3	1.59×10^{16}	S
0.5	19	11.5	Inf	Nan	−1	1.59×10^{16}	S
1	10.2	14.1	Inf	Nan	0	1×10^{9}	S

5	−6.75	18.3	26.7	16.1	10.5	20	*NS*
10	−13.2	19.1	39.4	15.9	16.5	20	*NS*
20	−19.5	19.5	45.6	15.8	22.3	20	*NS*

1.5.2 An innovative voltage-mode universal switched-capacitor filter's response to varying central frequency (f_o)

With circuit Q-factor=1, the circuit performance is examined for various center frequency values for low-pass (LP), band-pass (BP), and high-pass (HP) filters. This circuit's normal working range is between 10 Hz and 1.2 MHz. The value of ϵ $(\epsilon_1 = \epsilon_1 = \epsilon_1)$ is 2π (0.56) $\times 10^6$ rad/sec.

Table 1.6: Capacitors values for low-pass (LP) filter, with Q=1.

f_o (kHz)	C_1 (µf)	C_2 (µf)	C_3 (µf)	C_4 (µf)
220	53.8	24.8	6.06	15.4
225	54.6	25.8	6.49	13.2
230	55.3	26.8	6.93	10.9
235	56.1	27.8	7.39	8.68
240	56.9	28.9	7.87	6.41
250	58.3	31.01	8.90	1.82

Table 1.7: Capacitors values for band-pass (BP), and high-pass (HP)

المجلد(9) العدد(2) سبتمبر 2026م
https://doi.org/10.54582/TSJ.2.2.170

filters,

with Q=1.

f_o (kHz)	C_1 (f)	C_2 (f)	C_3 (f)	C_4 (f)
10	3.51 µ	63.21n	0.57 n	96.43 µ
20	6.89 µ	250.55n	4.56 n	92.85 µ
40	13.3 µ	983.97n	36.44n	85.68 µ
60	19.26 µ	2.17 µ	123 n	78.45 µ
80	24.78 µ	3.79 µ	291.6n	71.14 µ
200	50.47 µ	20.96µ	4.555 µ	24.02 µ

A. Low–Pass Filter Stability Response

Fig. 1.6 displays a low–pass (LP) filter's stability response for a range of f_o values. The information from the stability response curve study is presented in Table 1.8. With center frequencies of 210, 220, 230, 240, 250, and 260 kHz (all in kHz), the stability response is examined for merit factor Q=1. It can be seen from the stability response that the low–pass filter is effective for $f_o \geq 220\ kHz$. For $f_o \geq 220\ kHz$, regarding f_o, the gain margin has a positive value. The low–pass filter is therefore exceptionally reliable only over the frequency range of $220\ kHz \leq f_o \leq 250\ kHz$ with Q=1. When $f_o = 230\ kHz$, the stability

response is seen to have a phase margin of 35.5^0 at 246 kHz. With an increase in the center frequency value, the peak gain in relation to f_O drops. For example, the highest gain for f_O=220 kHz is 8.1 dB at 0.44 kHz whereas it is –13.8 dB at 0.5 kHz for f_O=250 kHz. As a result, the central frequency regulates the gain margin, the phase margin, and the peak gain.

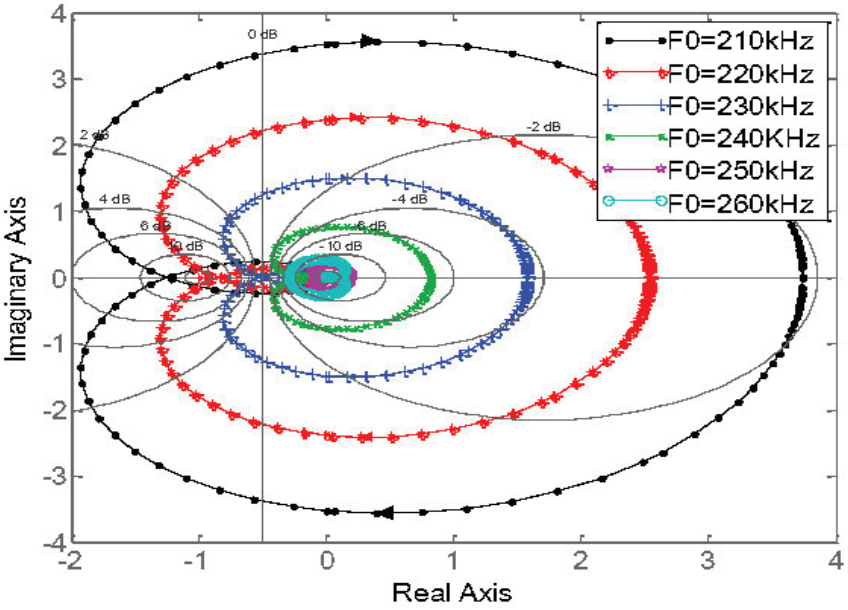

Fig. 1.6: Low-pass (LP) filter stability response, with Q=1.

Table 1. 8: Low-pass (LP) response graph analysis of Fig. 1.6.

f_O (kHz)	Gain-Margin (G_M)		Phase-Margin (P_M)		Peak-Gain		Stability Status
	(dB)	f_{GCO} (kHz)	(deg)	f_{PCO} (kHz)	(dB)	f_P (kHz)	

210	−192	297	−8.27	322	11.5	4.2×10^{-3}	*NS*
220	1.47	311	7.31	292	8.1	0.44	*S*
230	5.58	325	35.5	246	4	4.6×10^{-3}	*S*
240	11.3	339	Inf	Nan	−1.8	0.48	*S*
250	23.3	354	Inf	Nan	−13.8	0.5	*S*
260	10.9	0	Inf	Nan	−10.9	5.2×10^{-3}	*NW*

B. Band–Pass Filter Stability Response

For different values of f_o, the stability response of a band–pass (BP) filter is shown in Fig. 1.7. The information gleaned from analyzing the stability response curves seen in Fig. 1.7 is presented in Table 1.9. The band–pass filter is seen to function for $f_o \leq 250\,kHz$. Gain margin for all values of f_o is infinite dB. Therefore, for $f_o \leq 250\,kHz$ with Q=1, the band–pass filter is quite stable. Except for $f_o = 210\,kHz$, where the phase margin is 138^0 at 206 kHz, the stability response displays an infinite degree phase margin. The peak gain decreases as the value of f_o rises.

The max gain, for instance, is 0.174 dB at $f_o = 210\,kHz$ and –23.6 dB at $f_o = 250\,kHz$.

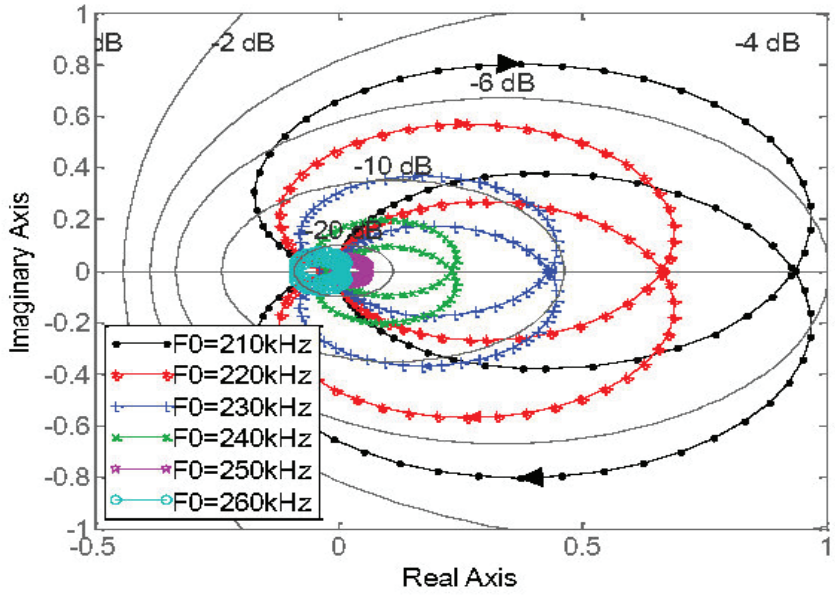

Fig. 1.7: Band-pass (BP) filter stability response, with Q=1.

Table 1. 9: Band-pass (BP) response graph analysis of Fig. 1.7.

f_O (kHz)	Gain-Margin (G_M)		Phase-Margin (P_M)		Peak-Gain		Stability Status
	(dB)	f_{GCO} (kHz)	(deg)	f_{PCO} (kHz)	(dB)	f_P (kHz)	
210	Inf	Nan	138	206	0.174	189	S
220	Inf	Nan	Inf	Nan	-2.8	198	S
230	Inf	Nan	Inf	Nan	-6.54	207	S

240	Inf	Nan	Inf	Nan	−11.9	216	S
250	Inf	Nan	Inf	Nan	−23.6	225	S
260	Inf	Nan	Inf	Nan	−20.3	234	NW

C. High–Pass Filter Stability Response

The stability response of a high–pass (HP) filter for different f_o values is shown in Fig. 1.8. Table 1.10 contains the data acquired from the analysis of the stability response curves shown in Fig. 1.8. It has been found that the high–pass filter also functions at $f_o \leq 250\ kHz$. As the value of f_o rises, the gain margin does as well. For example, for $f_o = 210\ kHz$, it is 23.6 dB at 148 kHz, while for $f_o = 250\ kHz$, it is 44.4 dB at 177 kHz. Because of this, the high–pass filter is only very reliable at $f_o \leq 250\ kHz$ with Q=1. the stability response exhibits an infinite–degree phase margin for all values of f_o.

With a rise in the central frequency value, the peak gain falls. For example, the gain margin for $f_o = 210\ kHz$ is −14.1 dB at $1.59\times10^{16} kHz$ and for $f_o = 250\ kHz$ is −34.8 dB at $7.85\times10^{17} kHz$.

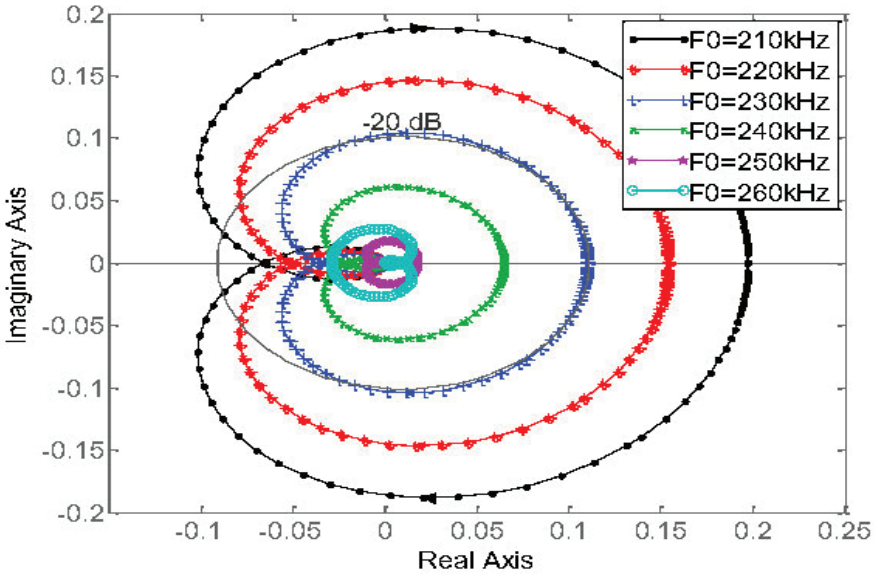

Fig. 1.8: High-pass (HP) filter stability response, with Q=1.

Table 1. 10: High-pass (HP) response graph analysis of Fig. 1.8.

f_O (kHz)	Gain-Margin (G_M)		Phase-Margin (P_M)		Peak-Gain		Stability Status
	(dB)	f_{GCO} (kHz)	(deg)	f_{PCO} (kHz)	(dB)	f_P (kHz)	
210	23.6	148	Inf	Nan	−14.1	1.59×10^{16}	S
220	25.8	156	Inf	Nan	−16.3	1.1×10^{10}	S
230	28.8	163	Inf	Nan	−19.2	1.15×10^{5}	S

https://doi.org/10.54582/TSJ.2.2.170

240	3 3.4	17 0	In f	N an	– 23.9	1.2× 10^5	S
250	4 4.4	17 7	In f	N an	– 34.8	7.85× 10^{17}	S
260	3 0.9	N AN	In f	N an	– 30.9	1.3× 10^{14}	NW

1.6 CONCLUDING REMARKS

In order to implement an innovative voltage–mode universal switched–capacitor filter with numerous feedback signals, a new circuit topology is proposed. Through one of the SCs, the terminals of the first and second operation–inverting amplifiers receive a low–voltage input signal. As a feedback network, the other three switched–capacitors are employed. The LP filter is only asymptotically stable for Q=1 and operates for Q1 in terms of quality factor. In contrast, with regard to central frequency, it operates for $f_o \leq 250\,kHz$ and is asymptotically stable only for $220\,kHz \leq f_o \leq 250\,kHz$. In terms of quality factor, the BP filter functions and is extremely stable for all values of Q. However, in terms of central frequency, it operates and is asymptotically stable for $f_o \leq 250\,kHz$. In terms of quality factor, with the exception of Q≤1, the HP filter operates and is asymptotically stable. In terms of central frequency, the HP filter operates and is asymptotically stable for $f_o \leq 250\,kHz$. Both narrow and large bandwidths can be employed with this filter. The circuit is not very sensitive to both active and passive components. The circuit concurrently performs the HP and BP transfer operations. For all values of Q and f_0, the circuit performs better in terms of BP. The

findings demonstrate that the circuit performs better for Q=1 in the LP and HP ranges. The benefit of RC–filter's stability response is that it makes sure the output signal stays within a specific range and doesn't fluctuate or diverge over time. This is crucial for a variety of applications that demand a consistent output signal, including audio processing, control systems, and communication systems. Additionally, a consistent filter response guarantees that the filter won't add any unwanted noise or distortion to the signal. Furthermore, a stable RC–filter response makes it simpler to analyze and build the filter since it eliminates mistakes in calculations and lowers the possibility of instability problems. Given is a PSPICE circuit simulation tool that supports the theoretical analysis.

1.7 RECOMMENDATIONS AND FUTURE WORK

Based on the findings of this study, the following recommendations are proposed for future research:

1. It is suggested that the proposed RC–filter topology be built using real electronic components to prove experimentally the validity of the theoretical and simulation findings.

2. The impact of temperature changes on the stability, center frequency, and Q–factor of the proposed filter under different operational conditions should be studied further.

3. Future research should investigate the behavior of the proposed filter under different power supply voltage changes to test its robustness and reliability.

4. The proposed filter should be compared with recently designed universal RC–filters in terms of complexity, power dissipation, sensitivity, stability, chip area, and overall performance.

5. Future research can include an expansion of the proposed topology to high-order filters (fourth and fifth order) in order to obtain better frequency selectivity.

6. A tolerance study needs to be performed to find out the effect of manufacturing tolerances in active and passive components on the filter performance.

7. Designing a low-power filter would make the proposed topology more useful for battery-operated devices, IoT, wearable electronics, and biomedical applications.

8. Verification through other circuit simulation software like MATLAB/Simulink, Cadence, or LT-spice is advisable in order to validate the designed circuit and to conduct a comparison of the results obtained.

9. Further studies can involve the practical implementation of the proposed circuit in real-life systems such as communication systems, biomedical signal processing, audio signal processing, and industrial control systems.

10. It is important that future researches focus on the influence of noise and harmonic distortion on the performance of the filter.

11. Electronic tuning of the center frequency and Q value can also be achieved with future study in order to enable automatic control without the need for modifying the passive components' values.

12. The circuit can also be realized in the form of a CMOS IC design with subsequent evaluation of chip area, power consumption, cost of production, and possibility of fabrication.

13. Monte Carlo Analysis can be conducted to analyze the statistical robustness of the designed circuit.

14. The practical application of the designed filter in RF communication systems can be studied further.

[8] Kacar F., Yesil A. & Noori A. (2012). New CMOS realization of voltage differencing buffered amplifier and its biquad filter applications. Radioengineering. 21(1), pp.333–339.

[9] Tarunkumar H., Ranjan A. & Pheiroijam N.M. (2018). Universal biquadratic filter with minimum number of active FTFN. Procedia Computer Science. 125, pp.818–824.

[10] Pathak J.K., Singh A.K. & Senani R. (2013). New voltage mode universal filters using only two CDBAs. International Scholarly Research Notices. 2013.

[11] Yuce E. (2017). A single–input multiple–output voltage–mode second–order universal filter using only grounded passive components. Indian Journal of Engineering and Materials Sciences. 24, pp.97–106.

[12] Roy S., et al. (2021). Voltage Differencing Current Conveyor Based Voltage–Mode and Current–Mode Universal Biquad Filters with Electronic Tuning Facility. International Journal of Engineering and Technology Innovation. 11(2), 146.

[13] Horng J.W. & Jhao Z.Y. (2013). Voltage–mode universal biquadratic filter using single DVCC. International Scholarly Research Notices. 2013.

[14] Ghausi M. (1984). Analog active filters. IEEE Transactions on Circuits and Systems. 31(1), pp.13–31.

[15] Shah N.A., Rather M.F. & Iqbal S.Z. (2006). SITO electronically tunable high output impedance current–mode universal filter. Analog Integrated Circuits and Signal Processing. 47, pp.335–338.

[16] Gupta M., Dogra P. & Arora T.S. (2019). Novel current mode universal filter and dual-mode quadrature oscillator using VDCC and all grounded passive elements. Australian Journal of Electrical and Electronics Engineering. 16(4), pp.220-236.

[17] Satansup J. & Tangsrirat W. (2014). Compact VDTA-based current-mode electronically tunable universal filters using grounded capacitors. Microelectronics Journal. 45(6), pp.613-618.

[18] Herencsar N., et al. (2015). Voltage-mode CFTA-C third-order elliptic low-pass filter design and optimization using signal flow graph approach. Elektronika ir Elektrotechnika. 21(2), pp.24-29.

[19] Paul T.K. & Pal R.R. (2019). Floating gate MOSFET based current differencing buffered amplifier and its applications as third-order filters. International Journal of Computational Engineering Research. 9(3), pp.53-61.

[20] Pandey N., Kumar P. & Paul S.K. (2015). Voltage differencing transconductance amplifier based resistorless and electronically tunable wave active filter. Analog Integrated Circuits and Signal Processing. 84, pp.107-117.

[21] Komanapalli G., Pandey N. & Pandey R. (2018). New realization of third order sinusoidal oscillator using single OTRA. AEU-International Journal of Electronics and Communications. 93, pp.182-190.

[22] Singla D.G. (2017). Design and Simulation of Third Order Low Pass Filter Using Operational Transconductance Amplifier. International Journal of Advanced Research in Electronics and Communication Engineering. 6(3), pp.188-190.

[23] Qasem A.A. & Shinde G.N. (2014). Third-Order Switched-Capacitor Tunable Bandwidth Filter with Multifunction Signal for Different Center Frequency (f0). International Journal of Electronic Networks, Devices, and Fields. 6(1), pp.1-10.

[24] Ranjan A., et al. (2017). Third order voltage mode universal filter using CCCII. Analog Integrated Circuits and Signal Processing. 90, pp.539-550.

[25] Phatsornsiri P., et al. (2014). Current-mode third-order quadrature oscillator using VDTAs and grounded capacitors. Proceedings of the 4th Joint International Conference on Information and Communication Technology, Electronic and Electrical Engineering (JICTEE). 2014.

[26] Channumsin O. & Jantakun A. (2014). Third-order sinusoidal oscillator using VDTAs and grounded capacitors with amplitude controllability. Proceedings of the 4th Joint International Conference on Information and Communication Technology, Electronic and Electrical Engineering (JICTEE). 2014.

[27] Chen H.P., et al. (2019). Electronically tunable third-order quadrature oscillator using VDTAs. Journal of Circuits, Systems and Computers. 28(4), pp.1950-1966.

[28] Chen H.P., Hwang Y.S. & Ku Y.T. (2018). A new resistorless and electronic tunable third-order quadrature oscillator with current and voltage outputs. IETE Technical Review. 35(4), pp.426-438.

[29] Shim Y. & Rais-Zaden M. (2012). A high-performance continuously tunable bandpass filter. IEEE Transactions on Microwave Theory and Techniques. 60(8).

[30] Kumngern M., Khateb F., Kulej T., & Knobnob B. (2024). 1 V Tunable High-Quality Universal Filter Using Multiple-Input Operational Transconductance Amplifiers. Sensors, 24(10), Article 3013.

[31] Dogan M., Yuce E., & Dicle Z. (2024). Voltage-Mode Multifunction and Universal Biquads with Two CFOAs. Journal of Circuits, Systems and Computers, 33(11), Article 2450196.

[32] Dogan M., Yuce E., & Minaei S. (2026). First-order Universal Filters with Two CCII+s and a Grounded Capacitor: Theory and Validation. Integration, the VLSI Journal, 107, Article 102642.

[33] Minayi E. (2025). A New Multi-Input Single-Output Voltage-Mode Universal Biquadratic Filter with Grounded Passive Elements and Orthogonally Adjustable Filter Parameters. Pamukkale University Journal of Engineering Sciences, 31(3), pp. 368-372.



Scientific Journal

of University of Saba Region

A Biannual Refereed Scientific Journal Issued by University of Saba Region

ISSN :2709-2747 (Online)

ISSN :2709-2739 (Print)

Volume 9, Issue 2, September , 2026